

# Has saturation physics been observed in deuteron-gold collisions at RHIC ?

Rudolf Baier<sup>a</sup>, Yacine Mehtar-Tani<sup>b</sup>, Dominique Schi<sup>b</sup>

<sup>a</sup>Fakultät für Physik, Universität Bielefeld,  
D-33501, Bielefeld, Germany

<sup>b</sup>Laboratoire de Physique Théorique, Université de Paris XI,  
Bâtiment 210, 91405 Orsay Cedex, France

## Abstract

In the framework of the recently proposed saturation picture, we examine in a systematic way whether the nuclear modification factor measured for d-Au collisions at RHIC may be simply explained. The Cronin peak which is obtained at mid-rapidity around  $k_T \approx 3$  GeV may be reproduced at the proper height only by boosting the saturation momentum by an additional nuclear component as already shown in the literature. In this respect, mid-rapidity RHIC data cannot necessarily be seen as a probe of the saturation picture. The large rapidity ( $|\eta| > 3$ ) region allows us to test the shape of the unintegrated gluon distribution in the nucleus, investigating various parameterizations inspired by large rapidity solutions (of the BFKL and) of the Balitsky-Kovchegov (BK) equation. A satisfactory description of  $R_{CP}$  at RHIC is obtained in the BK picture.

## 1 Introduction

Testing the saturation (Color Glass Condensate) picture [1], for the initial state of deuteron-gold (dA) collisions against RHIC data has been a subject of interest for some time. Two salient features have been observed [2, 3] concerning the behavior of the nuclear modification factor  $R_{dA}$ . At mid-rapidity, the Cronin peak height depends on the centrality of the collision. At large rapidity, the suppression predicted by quantum evolution is observed and is bigger for smaller centralities. A number of papers have recently discussed the description of the Cronin enhancement [4, 5, 6, 7, 8, 9] and the effect of small  $x$  [6, 10, 11, 12, 13, 14]. In this work, we examine in a systematic way, how and if saturation and quantum evolution provide a reasonable quantitative agreement with data [2].

The time is indeed appropriate to assess the predictability of the saturation (CGC) picture. This endeavor has a mitigated conclusion: as it turns, unavoidably, the saturation scale introduced in the theory, does not have the proper size to explain RHIC data at mid-rapidity. This conclusion is similar to the one stated in [5]. On the other hand, quantum evolution as described by the theory gives the proper suppression of the nuclear modification factor above the saturation scale.

---

E-mail address: mehtar@th.u-psud.fr

In section 2.1, we calculate the hadron production cross section in dA at mid-rapidity using the semi-classical approach and show the prediction for the minimum-bias nuclear modification factor  $R_{dA}$  (and  $R_{CP}$  for central versus peripheral collisions dA collisions) in relation with other previous studies and comparing with data.

We then discuss, in section 2.2, quantum evolution. We first derive the expression for the cross-section at leading log accuracy, including both gluon and quark distributions within the deuteron. This expression is identical to eq. (22) in [15]. We then present various parameterizations of the unintegrated gluon distribution in the nucleus, inspired by large rapidity solutions of the BK equation [16] and show the comparison with representative data [2]. In section 3, the conclusion and outlook are given.

## 2 Hadron production in dA

The nuclear modification factor  $R_{dA}$  and the  $R_{CP}$  (Central/Peripheral collisions) ratio are defined as

$$R_{dA} = \frac{1}{N_{coll}} \frac{\frac{dN^{dA \rightarrow hX}}{d^2k}}{\frac{dN^{pp \rightarrow hX}}{d^2k}}; \quad (1)$$

$$R_{CP} = \frac{N_{coll}^P \frac{dN^{dA \rightarrow hX}}{d^2k}}{N_{coll}^C \frac{dN^{pp \rightarrow hX}}{d^2k}}; \quad (2)$$

$k$  and  $y$  are respectively the transverse momentum and the pseudo-rapidity of the observed hadron.  $N_{coll}$  is the number of collisions in dA, it is roughly twice the number of collisions in pA (proton-Gold). The centrality dependence of  $R_{dA}$  is related to the dependence of  $N^{dA \rightarrow hX} = \frac{dN^{dA \rightarrow hX}}{d^2b}$  and  $N_{coll}(b)$  on the impact parameter of the collision. In this paper, we address the predictions of the Color Glass Condensate for these ratios. We always assume that cross-sections depend on the impact parameter only through the number of participants which is proportional to the saturation scale

$$Q_{SA}^2(b) \propto Q_{SA}^2(0) N_{partAu}(b) = N_{partAu}(0); \quad (3)$$

where  $N_{partAu}$  is the number of participants in the gold nucleus in dAu collisions. This is coherent with the assumption that  $Q_{SA}^2(b) \propto (N_{partAu}(b)/2) Q_{sp}^2$  such that  $Q_{SA}^2(b=0) \propto A^{1/3} Q_{sp}^2$  [17]. We use Table 2 in [2] which gives the number of participants  $N_{part}$  and the number of collisions  $N_{coll}$  for several centralities.

### 2.1 Semi-classical approach

We first deal with gluon production at mid-rapidity for which different approaches have been proposed. The inclusive cross section has been calculated in [18] in a quasiclassical approach of multiple rescattering inside the nucleus, see also [6, 10]. Further confirmation has been given in [14, 19]. The inclusive cross section, for a gluon with transverse momentum  $k$  and rapidity  $y=0$ , is written as

$$\frac{d^{dA \rightarrow gX}}{d^2k d^2b} = \frac{C_F}{s} \frac{1}{(2)^3 k^2} \int^Z d^2B \int^Z d^2z r_z^2 n_G(z; b-B) r_z^2 N_G(z; b) e^{ik \cdot z}; \quad (4)$$

where  $N_G(z; b)$  is the forward scattering amplitude of a gluon dipole on the nucleus, it contains all higher twists in the semi-classical approximation and  $n_G(z; b-B)$  is the forward scattering amplitude of a gluon dipole on the deuteron at leading twist approximation.  $B$  and  $b$  are the impact parameters of the deuteron and the gluon with respect to the center of the nucleus. At mid-rapidity and RHIC energies, it is legitimate to neglect quantum evolution.

This approach provides a description of  $N_G$  at all orders in terms of the saturation scale  $Q_{sA}^2 = Q_s^2 A^{1/3} = Q_{CD}^2$ . The CGC approach yields a Glauber-Mueller form for the dipole forward scattering amplitude

$$N_G(z; b) = 1 - \exp\left(-\frac{1}{8}z^2 Q_s^2(b) \ln \frac{1}{z^{2-2\epsilon}}\right); \quad (5)$$

where the saturation scale is given by [18]

$$Q_s^2(b) \ln \frac{1}{z^{2-2\epsilon}} = \frac{4}{C_F} \frac{s}{z^2} T(b) x G(x; 1=z^2); \quad (6)$$

is the nuclear density in the nucleus and  $T(b) = \int_0^R \frac{R^2 - b^2}{R^2} b^2 db$  the nuclear profile function of a spherical nucleus of radius  $R$ .  $\epsilon$  is an infrared cut-off of order  $Q_{CD}$ . The cross section can be rewritten in the following simpler form

$$\frac{d^2 A^{\text{hX}}}{d^2 k d^2 b} = \frac{C_F}{z^2} \frac{s}{k^2} \int_0^Z \frac{1}{u} du \ln \frac{1}{u} \mathcal{E}_u [u \mathcal{E}_u N_G(u; b)] J_0(k_\perp u); \quad (7)$$

where  $u = |k_\perp|$ .

### 2.1.1 A model for minimum bias collisions

One defines the minimum bias cross-section as the average over the impact parameter of the collision, it may be written as

$$\frac{dN^{\text{min bias}}}{d^2 k} = \int \frac{d^2 b}{S_A} \frac{d^2 A^{\text{hX}}}{d^2 k d^2 b}; \quad (8)$$

$S_A = R^2$  is the transverse area of the nucleus. All the centrality dependence in the cross-section is contained in  $N_G(z; b)$  as given by (5) and (6). One can perform the  $b$  integral for  $N_G$  yielding

$$\langle N_G(z; Q_s) \rangle = 1 + \frac{128}{z^4 Q_{sC}^4 \ln^2(1=z^{2-2\epsilon})} \left[ \left(1 + \frac{1}{8}z^2 Q_{sC}^2 \ln(1=z^{2-2\epsilon})\right) \exp\left(-\frac{1}{8}z^2 Q_{sC}^2 \ln(1=z^{2-2\epsilon})\right) - 1 \right]; \quad (9)$$

where  $Q_{sC}^2 = Q_s^2(b=0)$ . The corresponding result for  $R_{dA}$  is shown in Fig. 1 (a) taking  $Q_{sC}^2 = 2 \text{ GeV}^2$  and  $\epsilon = 0.2 \text{ GeV}$ . The proton-proton cross-section is calculated by using the Glauber-Mueller formula (5) with  $Q_{sp} \cdot R_{dA}$  shows a Cronin peak for  $k_\perp$  in the range of  $Q_s$ . We have used a prescription such that the region  $z \ll 1$  does not affect the integral. For that purpose, we make the replacement  $\ln \frac{1}{z^{2-2\epsilon}} \rightarrow \ln \left(\frac{1}{z^{2-2\epsilon}} + a^2\right)$  choosing  $a = 3$  [4]. A good approximation of the integral over  $b$  is to choose for  $Q_s$  the average value  $\langle Q_s^2(b) \rangle = Q_{s \text{ min bias}}^2 = (2/3)Q_{sC}^2$ , in which case

$$\int \frac{d^2 b}{d^2 k d^2 b} (Q_s^2(b)) \approx \frac{d^2 A^{\text{hX}}}{d^2 k d^2 b} (Q_s^2(b)); \quad (10)$$

Actually, (10) turns into an equality in the high  $k_\perp$  region and is quite good in the region of the Cronin peak. In Fig. 1 (b) we see that the error is maximum when  $k_\perp \sim Q_s$ , reaching 10%. For a cylindrical nucleus there is no  $b$  dependence in the cross section and (10) turns into an equality. This tells us that the physics is the same whatever the geometry of the nucleus [6].

### 2.1.2 Effects of fragmentation on the Cronin peak

To get the hadron cross-section we still have to convolute (7) with the proper fragmentation functions

$$\frac{d^2 A^{\text{hX}}}{d^2 k d^2 b} = \int \frac{dz}{z^2} D_g^h(z; Q_f^2) \frac{d^2 A^{\text{hX}}}{d^2 q d^2 b} (q = k/z); \quad (11)$$

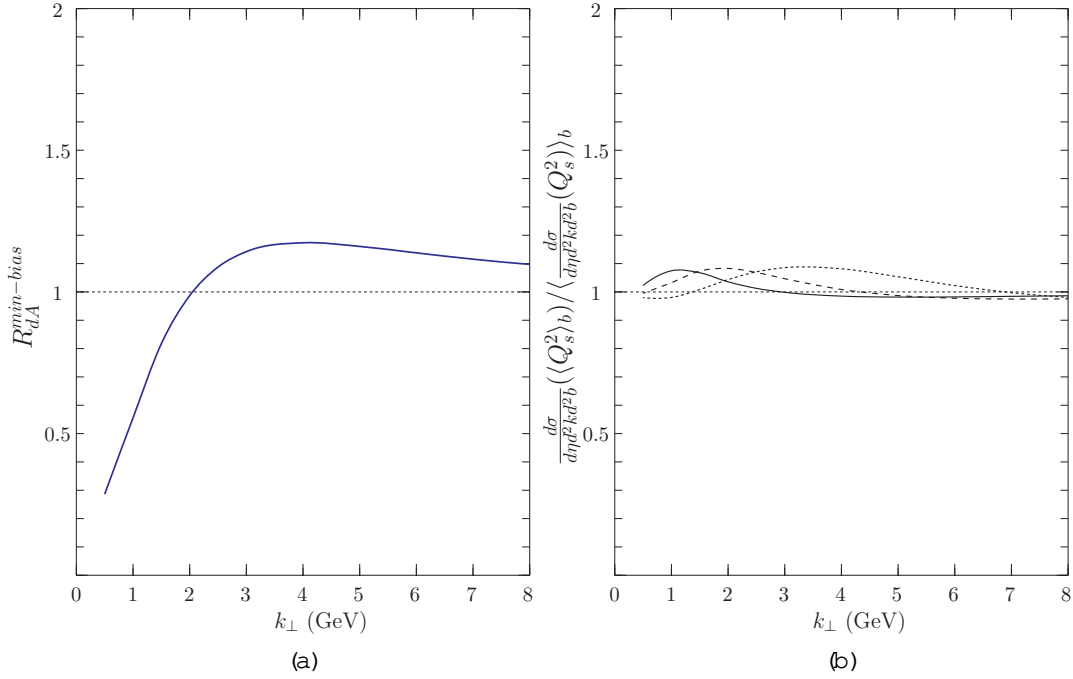


Figure 1: (a): The nuclear modification factor  $R_{dA}$  without fragmentation functions (gluon production) for  $Q_{SC}^2 = 2 \text{ GeV}^2$ . (b): Comparison between the average full min-bias calculation and the calculation with average min-bias  $Q_s$  for  $Q_{SC}^2 = 2, 5$  and  $9 \text{ GeV}^2$  (Full, dashed and dotted).

where  $Q_f$  is a large scale of order  $k_{\perp}$  taken between 2 and 8 GeV. We use the fragmentation functions of [20]. In Fig 2 (a) we present the result for  $R_{dA}$ .

The fragmentation functions induce a flattening of the Cronin peak toward 1, with a shift toward the small  $k_{\perp}$ 's. This feature can be understood by comparing  $R_{dA}^g$  without FF's (fragmentation functions) and  $R_{dA}^h$  with FF's, order by order in powers of  $Q_s^2 = k^2$  (or the number of participants). Above the saturation scale, the following expansion has a meaning

$$R_{dA}^g = 1 + R_{dA}^{(1)g} + \dots \quad (12)$$

In the Leading Log approximation with respect to  $\ln(k_{\perp})$ , using (11), we approximate the nuclear modification factor by

$$R_{dA}^h = 1 + \frac{hz^4i}{hz^2i} R_{dA}^{(1)g} + \dots \quad (13)$$

where we have defined for  $n > 2$

$$hz^n i = \int_{z_0}^{Z_1} dz D(z; Q_f^2) z^n = \int_{z_0}^{Z_1} dz D(z; Q_f^2): \quad (14)$$

Since  $z < 1$  we always have  $hz^n i = hz^2 i < 1$ . The rescattering terms are then less important and  $R_{dA}^h$  gets closer to 1. This is shown in Fig. 2 (a): comparing with Fig. 1 (a) we see the dramatic effect of the fragmentation functions for  $Q_{s \text{ min-bias}}^2 = 1.3 \text{ GeV}^2$ . To get agreement with RHIC data we have to increase the value of the saturation scale  $Q_s$  and take  $Q_{s \text{ min-bias}}^2 \approx 6 \text{ GeV}^2$ . This feature has already been mentioned in [7]. In fact,  $Q_s^2$  as defined in (6) is at most of the order of  $2 \text{ GeV}^2$  for  $b = 0$ . The

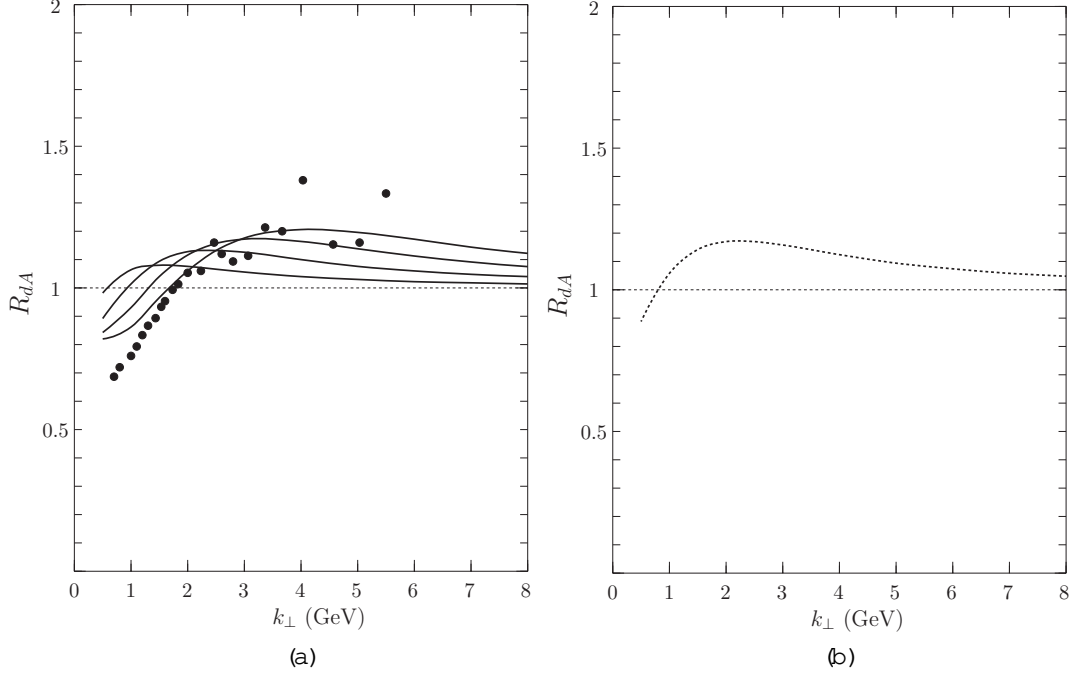


Figure 2: (a): Minimum bias  $R_{dA}$  for charged hadron production for  $Q_{s\text{ in bias}}^2 = 1; 3; 3.3; 6$  and  $9 \text{ GeV}^2$  (lowest to highest curve). (b): Minimum bias  $R_{dA}$  for neutral pion production for  $Q_{s\text{ in bias}}^2 = 9 \text{ GeV}^2$ . The points are representative data taken from [2].

authors of [7] propose to enhance it by adding an additional momentum due to "non-perturbative" nuclear effects:

$$Q_s^2 \rightarrow Q_s^2 + \Lambda^2 A^{1/3}; \quad (15)$$

with  $\Lambda^2 = 1 \text{ GeV}^2$ . This amounts to boosting  $Q_s^2(b=0)$  to  $9 \text{ GeV}^2$ . In fact, as shown in Fig. 2 (a), we need even a larger saturation scale. On the other hand, the way  $R_{dA}$  is normalized (by estimating the proton-proton cross-section using (5)) is not fully convincing. The ratio  $R_{CP}$  does not suffer from the same uncertainty. It is shown in Fig. 3 for  $Q_{sC}^2 = 9 \text{ GeV}^2$  and  $Q_{sC}^2 = 2 \text{ GeV}^2$  for central and semi-central collisions. Taking into account the experimental error-bars, the large value for  $Q_{sC}$  is definitely preferred and in agreement with data.

We should at this point remark that saturation physics in the present stage is in the situation where the leading order perturbative QCD description was, concerning large  $k_T$  spectra in hadron-hadron collisions. The agreement with data could only be obtained by implementing an intrinsic non-perturbative transverse momentum for partons inside the hadron. The present state seems to be that, at next-to-leading order, the perturbative theory becomes predictive [21]. In this respect and in the leading order perturbation QCD framework, the authors of ref. [5] have used a traditional Glauber-Eikonal approach of sequential multiple partonic scatterings with the implementation of a large intrinsic  $k_T$  in parton distribution functions and they have obtained a good agreement with data for  $\phi$  production in dA collisions.

Staying in the saturation physics framework, we may nonetheless try to go beyond the ad-hoc ansatz (15) and modify the saturation picture, which is exclusively based on hard multiple scatterings, by adding non-perturbative scatterings, when a parton (gluon) is passing through a nucleus. Following

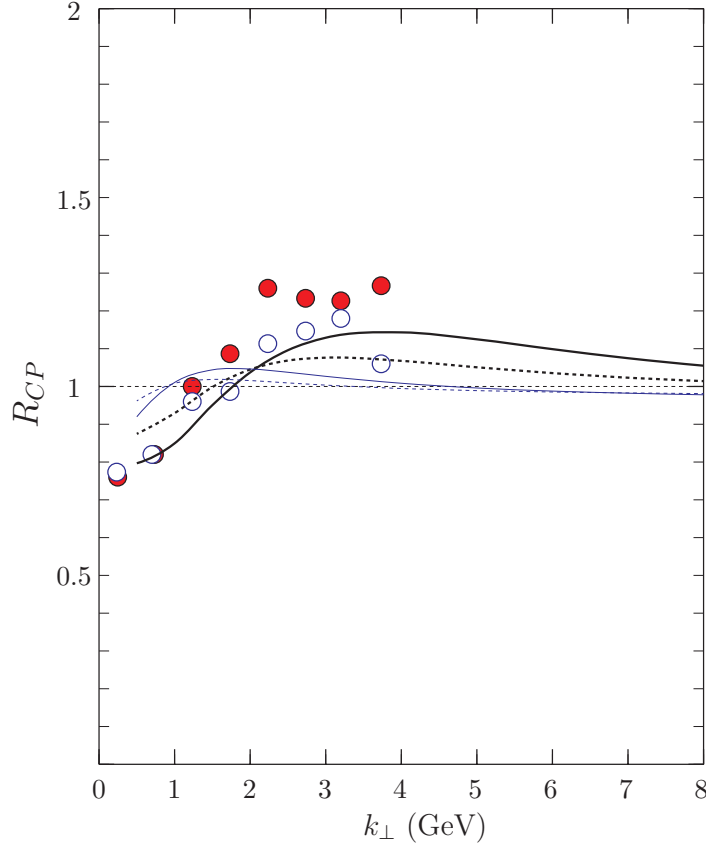


Figure 3:  $R_{CP}$  for  $Q_{s,c}^2 = 9 \text{ GeV}^2$  (thick lines) and  $Q_{s,c}^2 = 2 \text{ GeV}^2$  (thin lines). Full lines correspond to central over peripheral collisions (full experimental dots). Dashed lines correspond to semi-central over peripheral collisions (empty experimental dots). Data from [2].

the Moliere scattering theory [22] extended to QCD [23], we define the probability distribution for the scattered parton by

$$V(k) = \frac{1}{d^2k} = \frac{1}{f} \frac{c}{hk^2 i} e^{-\frac{k^2}{hk^2 i}} + \frac{(1-c)^2}{(k^2 + \frac{1}{2})^2} g; \quad (16)$$

with  $\int d^2k V(k) = 1$ .

A soft, non-perturbative, gaussian contribution is added to the hard screened (by mass) gluon exchange term. Solving the kinetic master equation for the survival probability of the propagating parton, an effective scale (up to logarithm) is derived,

$$Q_s^2 \rightarrow (c \frac{hk^2 i}{2} + (1-c)Q_s^2); \quad (17)$$

Different from (15) the non-perturbative part is added but weighted by a factor  $c < 1$ .

In order to obtain an effective  $Q_s^2 \approx 0$  ( $10 \text{ GeV}^2$ ) one has to add a significant non-perturbative part, e.g. for  $hk^2 i = 0.5 \text{ GeV}^2$ ,  $c = 0.2 \text{ GeV}$  and  $c' = 0.3$  indeed

$$Q_s^2 \approx 2 \text{ GeV}^2 \rightarrow Q_s^2 \approx 9 \text{ GeV}^2; \quad (18)$$

The underlying picture of dominating soft parton interactions with nucleons has strong implications, especially for the width of jet broadening, i.e. the resulting transport coefficient for cold matter  $\hat{q} \propto Q_s^2 = (2R)^{-2}$  becomes also rather large, namely  $\hat{q} \approx 0.8 \text{ GeV}^2/\text{fm}$  (for gold)! But such a strong jet broadening has not been observed so far [24].

## 2.2 Forward rapidity and quantum evolution

### 2.2.1 Hadron production cross-section

As shown in [6], it is possible to rewrite eq. (4) under a  $k_T$ -factorized form, which is then generalized to include the rapidity dependence. Denoting the unintegrated gluon distribution for the nucleus and the deuteron, respectively, as

$$\mathcal{F}_A(Y_A; k; b) = \frac{C_F}{s(2)^3} \int_0^Z dz z r_z^2 n_G(Y_A; z; b) e^{ik_z z}; \quad (19)$$

and

$$\mathcal{F}_p(Y_d; k; b) = \frac{C_F}{s(2)^3} \int_0^Z dz z r_z^2 n_G(Y_d; z; b) e^{ik_z z}; \quad (20)$$

with  $Y_A = \ln(1/x_A) = Y + \ln 2$  and  $Y_d = \ln(1/x_d) = Y$  the rapidities of the gluons merging respectively from the nucleus and the deuteron and carrying the light cone momentum fractions  $x_A$  and  $x_d$ ;  $Y$  is the rapidity of the produced gluon measured in the forward deuteron direction and  $Y = \ln(\sqrt{s}/k_T)$ . One obtains the expression for the cross-section as

$$\frac{d^4 \sigma}{d^2 k d^2 b} = \frac{2}{C_F} \frac{1}{k^2} \int_0^Z dz B \int_0^Z dz' q_d(q; k; Y + \ln 2; b) \mathcal{F}_A(q; Y + \ln 2; b); \quad (21)$$

Whereas (4) incorporates all twists for the nucleus wave function in the semi-classical approach, (21) is only valid at leading twist. We will focus our analysis on the large forward rapidity region for the gluon where we can neglect the emission of additional gluons in the wave function of the proton. Actually, in this region the biggest value of  $Y_d$  is reached at  $b = 0$  yielding  $Y_d = Y$  which is not indeed large enough at the energies of RHIC for the evolution to take place. However, the opposite happens in the nucleus where  $Y_A$  increases with  $b$  and we thus expect to probe the small  $x$  regime of the nucleus wave function. We have, taking  $\mathcal{F}_d \approx \mathcal{F}_p$  at leading twist without quantum evolution [18],

$$\int_0^Z dz b \mathcal{F}_d(k; Y + \ln 2; b) = \frac{s C_F}{k^2} \frac{2}{k^2}; \quad (22)$$

This allows us, assuming  $\mathcal{F}_A$  smooth enough, to approximate (21) at leading log accuracy, when  $k_T \ll \sqrt{s}$ , by

$$\frac{d^4 \sigma}{d^2 k d^2 b} = \frac{2}{C_F} \frac{\mathcal{F}_A(k; Y + \ln 2; b)}{k^2} \int_0^Z dz B \int_0^Z dz' q_d(q; Y + \ln 2; B) \mathcal{F}_p(q; Y; b); \quad (23)$$

Using the relation,

$$x_G(x_d; k^2) = \int_0^Z dz B \int_0^Z dz' q_d(q; Y + \ln 2; B) \frac{d^2 q}{k^2}; \quad (24)$$

we end up with

$$\frac{d^4 \sigma}{d^2 k d^2 b} = \frac{s(2)}{C_F} \frac{\mathcal{F}_A(k; Y + \ln 2; b)}{k^2} x_G(x_d; k^2); \quad (25)$$

Notice the collinear factorization of the gluon distribution in the proton. For hadron production one has to add the valence quark contribution which may be written [8]

$$\frac{d^4 A \rightarrow qX}{d^2 k d^2 b} = \frac{s(2)}{N_c} \frac{f_A(k; Y + \frac{1}{2} \ln z; b)}{k^2} x_{qV}(x_d; k^2); \quad (26)$$

Convoluting with the fragmentation functions we get

$$\frac{d^4 A \rightarrow hX}{d^2 k d^2 b} = \frac{s(2)}{C_F} \sum_{i=g,u,d} \int_{z_0}^1 dz \frac{f_A(k=z; Y + \frac{1}{2} \ln z; b)}{k^2} [f_i(x_d=z; k^2=z^2) D_{h=i}(z; k^2)]; \quad (27)$$

where  $f_{u,d}(x; k^2) = (C_F/N_c) x q_{1,d}(x; k^2)$  and  $f_g(x; k^2) = xG(x; k^2)$  are the parton distributions inside the proton;  $D_{h=i}(z; k)$  are FF's of the parton  $i$  into hadron  $h$ , and  $z_0 = (k_T^2 = \bar{s})e$ . Notice that this formula is identical to eq. (22) of [15] in the leading twist approximation. At forward rapidity, the longitudinal momentum fraction  $x_d$  carried by the parton inside the deuteron is of order of one. This implies that the dynamics of the deuteron is completely dominated by valence quarks. For numerical calculations we use the GRV LO parton distribution functions inside the proton from [25], assuming that there is no significant difference between the proton and the neutron for charged hadron production.

### 2.2.2 The unintegrated gluon distribution

In the physics of saturation the relevant observable is the forward scattering amplitude of a quark-antiquark dipole on a target (a nucleus in our case). It enters several processes at high energy like DIS, photoproduction and hadron-hadron scattering. Its quantum evolution has recently been the object of many studies [6, 10, 16, 27, 28, 29, 30]. We focus on the Balitsky-Kovchegov (BK) equation [16] valid in the large  $N_c$  limit and in the mean field approximation. It provides a tool to study the rapidity behavior of the gluon distribution near (above and not too far from) the saturation scale where the effects of gluon recombination, taken into account in the non-linear term, become important, instead of the BFKL equation [31] which contains only gluon splitting (linear term) yielding a power growth of the gluon distribution with respect to the center of mass energy violating unitarity and the Froissart bound. The BK equation reads in momentum space

$$\partial_Y N(k; Y) = \frac{N_c}{\partial \ln k^2} \left[ \left( \frac{\partial}{\partial \ln k^2} \right) N(k; Y) - N^2(k; Y) \right]; \quad (28)$$

where  $\left( \frac{\partial}{\partial \ln k^2} \right) = 2 \left( 1 - \left( \frac{\partial}{\partial \ln k^2} \right) \right)$  is the BFKL kernel, and

$$N(k; b; Y) = \frac{d^2 Z}{Z^2} N(z; b; Y) e^{izk}; \quad (29)$$

At large  $Y$ , a solution has been found for the BK equation near the saturation scale in terms of travelling waves. It has a geometric scaling behavior in the variable  $L = \ln(k^2/Q_s^2(b; Y))$  when  $Y$  goes to infinity [27, 29]

$$N(L; Y) = C L \exp[-s L - \frac{1}{2} (Y) L^2]; \quad (30)$$

$C$  is an undetermined constant irrelevant in the present analysis of  $R_{dA}$  and  $R_{CP}$ ,  $s = 0.628$  is the anomalous dimension of the BFKL dynamics in the geometric scaling region [29, 30]:  $Q_s^2 \propto k_T^2$ .  $Q_s^2(Y) \exp(1 - \frac{1}{2} (Y)) = (2^{-\frac{1}{2} (Y)})^{-1}$ . We used the recent fit to the HERA data performed in [32] where  $\frac{1}{2} (Y) = (2 - Y)^{-1}$ ,  $\frac{1}{2} = 0.25$ ,  $\frac{1}{2} = 9.9$  and  $Q_s^2(Y; 0) = 3 = 2Q_{s,m \text{ in bias}}^2(Y) = 3 = 2A^{1=3} (x_0 = x)$  GeV<sup>2</sup> with  $x_0 = 0.67 \pm 0.4$  and  $x = e^Y$  given here by  $x = k_T^2 = \bar{s} e$ . There is no straightforward way to link this asymptotic form to the one at mid-rapidity: this implies that there is an overall constant coming from  $Q_s$  which is negligible at very large rapidity and far from the saturation scale. We expect

this constant to play a significant role at RHIC energies. Then, one can fix  $Q_s$  as shown above, and put all the freedom into an additional constant ( $L \rightarrow L + L_0$ ). Thus,

$$N(L; y) = C^0 (L + L_0) \exp[-(s + 2L_0)L - L^2]: \quad (31)$$

Making the same approximations as in the BK equation, one can write an expression for  $N_G$  [6]

$$N_G(z; y) = \frac{2C_F}{N_c} (2N(z; y) - N^2(z; y)): \quad (32)$$

In the leading twist approximation where one can neglect non-linear terms, we find

$$N_G(z; y) \approx 2N(z; y): \quad (33)$$

Both distributions  $N$  and  $N_A$  are linked to the dipole scattering amplitude in (29) and (19). One can thus eliminate the latter yielding

$$N_A(L; y) = \frac{4N_c}{s(2)^3} \frac{d^2}{dL^2} N(L; y): \quad (34)$$

At very large  $y$  one can neglect the term which breaks scaling, namely  $L$ . So that the last expression reduces to the simple form exhibiting an exact scaling behavior

$$N_A(L; y) \approx (L + L_0 - \frac{2}{s}) \exp[-sL]: \quad (35)$$

We have fixed  $L_0$  such that  $N_A$  has a maximum when  $k^2 = Q_s^2(y)$  [29, 33] corresponding to  $L_0 = 3/s$ . This is the only free parameter of our calculation, it exhibits the uncertainty in the value of  $Q_s$ . It turns out that  $R_{CP}$  is very sensitive to variations of  $L_0$  at energies of RHIC. For the numerical study we choose three different expressions for  $N_A$ , selecting various specific terms in (31):

i) The BFKL saturation-inspired form [30], which violates scaling, derived from

$$N(L; y)_{\text{BFKL}} \approx \exp[-sL - L^2]: \quad (36)$$

ii) The BK exact-scaling form (35).

iii) Finally the full expression derived from (31).

In Fig. 4 we show the comparison between the BFKL + saturation form (36) and the BK parametrization (31). We expect this comparison to be valid at large enough  $k_T$ . The agreement with data is quite good for the latter. With decreasing rapidity we would expect our formula to break down, nevertheless the global features of the data are reproduced even at  $y = 1$ . The exact scaling form, shown in Fig. 5, is a slowly varying function of  $y$  and is too low to describe the data. However, if the picture is right, for increased rapidity ( $y \approx 5$  or 6), data points should match that shape. The fact that the saturation model has a semi-quantitative agreement with data for  $R_{CP}$  is essentially due to the anomalous dimension since an approximate form is (when  $k_T \approx Q_s$ )

$$R_{CP} \approx \frac{N_{\text{coll}}^P}{N_{\text{coll}}^C} \left( \frac{N_{\text{part}}^C}{N_{\text{part}}^P} \right)^{\text{eff}} \approx \left( \frac{N_{\text{part}}^C}{N_{\text{part}}^P} \right)^{\text{eff} - 1}: \quad (37)$$

At forward rapidity  $\text{eff} \approx s + (\ln(k_T^2/Q_s^2))$  is a decreasing function of  $y$  and an increasing function of  $k_T$ . This allows us to understand the qualitative behavior shown by data and in particular the inversion of the centrality dependence compared to mid-rapidity where  $R_{CP} \approx 1$  (Cronin enhancement) corresponding to  $\text{eff} \approx 1$ . At very large  $y$  the anomalous dimension stabilizes at  $\text{eff} = s$ , which could be tested at the LHC.

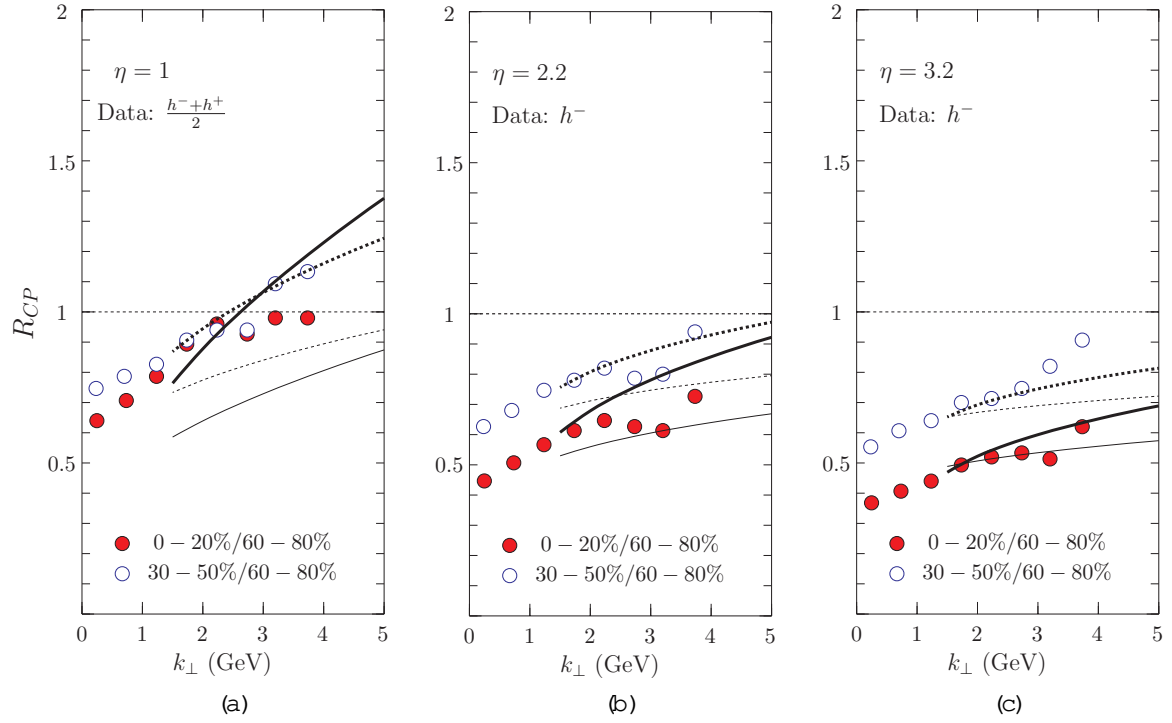


Figure 4:  $R_{CP}$  for the BK parametrization (thick lines) and the BFKL+saturation form (thin lines) at different rapidities  $\eta = 1, 2.2$  and  $3.2$ . Full lines correspond to central over peripheral collisions (full experimental dots). Dashed lines correspond to semi-central over peripheral collisions (empty experimental dots). Data from [2].

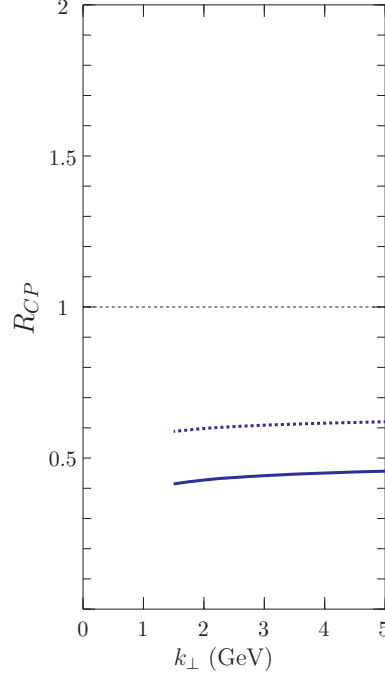


Figure 5:  $R_{CP}$  for the exact scaling BK form at  $\alpha_s = 3/2$ . Full line: central/peripheral, dashed line: semi-central/peripheral.

### 3 Conclusion and outlook

To conclude we may reiterate that in our opinion, the saturation picture as probed by mid-rapidity data for the nuclear modification factor at RHIC energies cannot be seen as predictive. Indeed, the CGC at mid-rapidity is based on leading order pQCD calculations including multiple eikonal partonic rescatterings inside the nucleus, giving rise to a saturation scale  $Q_s^2$  at most of order of  $2 \text{ GeV}^2$  and it turns out that this is not sufficient to describe RHIC data at mid-rapidity. It may be very interesting to relate the increase of the saturation scale needed to explain the dA data to the comparison of experimental measurements with theory for observables such as jet broadening in nucleus-nucleus (AA) collisions and also jet quenching, since the saturation scale determines their order of magnitude.

At forward rapidity, a saturation inspired framework for quantum evolution predicts the suppression as observed in data. This is a leading twist effect driven by the anomalous dimension which is the main source of the observed behavior. There is good evidence that the answer to the question: "has saturation been observed at RHIC?" is positive and a definitive answer could be provided if one measures, in a more precise way, the anomalous dimension as predicted by the theory. To do so, one needs to go to larger rapidities (energies) at LHC.

As one more step to improve further the status of the present theoretical description let us remark that initial state suppression effects may be also present in AA collisions at large  $\eta$  and large transverse momentum  $k_T$ . An interesting quantity to be measured is the double ratio  $R(\eta_1; \eta_2; k_T)$  with  $\eta_1 > \eta_2 > 0$ , defined by

$$R(\eta_1; \eta_2; k_T) = \frac{R_{CP}(\eta_1; k_T)}{R_{CP}(\eta_2; k_T)}; \quad (38)$$

as a function of  $k_T$ . For  $\eta_1 = 2.2$  and  $\eta_2 = 0$ , this ratio is measured for AA by the BRAHMS Collaboration [34]; there is evidence of suppression becoming more important at forward rapidities, as observed in dA measurements.

Because of the final state suppression in AA collisions one may argue that this ratio is bounded by

$$R(\eta_1; \eta_2; k_T) < R(\eta_1; \eta_2; k_T)_{\text{initial}} < 1; \quad (39)$$

where  $R(\eta_1; \eta_2; k_T)_{\text{initial}}$  for AA collisions may be estimated for  $R_{CP}$  initial in a way done for dA collisions (e.g. by assuming  $k_T$  factorization). We expect it to be quantitatively similar to the dA case (e.g. Figs. 4(b) and (c)), which is well understood in the saturation picture for  $\eta_1 > \eta_2 > 0$ . The inequality (39) is based on the assumption that  $R_{CP}$  in AA collisions may be factorized as  $R_{CP} \text{ initial } Q(k_T; \eta)$ : the quenching factor takes into account the (radiative) final state interactions [35]. It depends, at fixed  $k_T$  on the pathlength of the parton propagating in a dense medium, such that  $Q$  is decreasing with increasing pathlength, i.e. it amounts to more quenching. Assuming, on geometrical grounds, a longer path for  $\eta_1$  than for  $\eta_2$ ,  $\eta_1 > \eta_2$ , implies  $Q(k_T; \eta_1) = Q(k_T; \eta_2) < 1$ , and (39) follows.

## References

- [1] See the recent reviews "Saturation physics and Deuteron-Gold Collisions at RHIC", J.Jalilian-Marian and Y.V.Kovchegov, arXiv:hep-ph/0505052; J-P.Blaizot and F.Gelis, Nucl.Phys.A 750, 148 (2005); E.Iancu and R.Venugopalan, in "Quark Gluon Plasma 3". (editors: R.C.Hwa and X.N.Wang, World Scientific, Singapore), p.249-363, arXiv:hep-ph/0303204.
- [2] I.Arsene et al. [BRAHMS Collaboration], Phys.Rev.Lett. 93, 242303 (2004); R.Debbe for the BRAHMS Collaboration, arXiv:nuclex/0405018.
- [3] J.Adam et al. [STAR Collaboration], arXiv:nuclex/051009; B.B.Back et al. [PHOBOS Collaboration], arXiv:nuclex/0410022; K.Aldox et al. [PHENIX Collaboration], arXiv:nuclex/0410003; I.Arsene et al. [BRAHMS Collaboration], arXiv:nuclex/0410020.
- [4] R.Baier, A.Kovner and U.A.Wiedemann, Phys.Rev.D 68, 054009 (2003).
- [5] A.Accardi and M.Gyulassy, Phys.Lett.B 586, 244-253 (2004); A.Accardi, Acta.Phys.Hung. (to appear).
- [6] D.Kharzeev, Y.V.Kovchegov and K.Tuchin, Phys.Rev.D 68, 094013 (2003).
- [7] D.Kharzeev, Y.V.Kovchegov and K.Tuchin, Phys.Lett.B 599, 23-31 (2004).
- [8] F.Gelis and J.Jalilian-Marian, Phys.Rev.D 67, 074019 (2003).
- [9] E.Iancu, K.Itakura and D.N.Triantafyllopoulos, Nucl.Phys.A 742, 182-252, (2004).
- [10] Y.V.Kovchegov, K.Tuchin, Phys.Rev.D 65, 074026 (2002).
- [11] J.L.Albacete, N.Amesto, A.Kovner, C.A.Salgado and U.A.Wiedemann, Phys.Rev.Lett. 92, 082001 (2004).
- [12] J.Jalilian-Marian, Nucl.Phys.A 748 664-671 (2005).
- [13] D.Kharzeev, E.Levin and L.D.McLerran, Phys.Lett.B 561, 93 (2003).
- [14] J-P.Blaizot, F.Gelis and R.Venugopalan, Nucl.Phys.A 743, 13-56 (2004).

